Jitendra V. Dave Ralph Bernstein Harwood G. Kolsky

Importance of Higher-Order Components to Multispectral Classification

A Landsat multispectral image was combined with the corresponding digital terrain elevation data to study several information extraction procedures. Principal component and limited multispectral classification procedures were conducted on 1024×1024 four-band Landsat and five-band (Landsat plus terrain data) images, and color composites as well as quantitative information were generated. Selected results of this preliminary investigation confirm the usefulness of the principal component analysis in a qualitative presentation of the multi-band data and its association with a significant reduction in dimensionality. However, unlike some other investigators, we found that the full dimensionality must be retained when the information content of the data has to be preserved quantitatively.

Introduction

A single-band digital image generally consists of a 6to-8-bit representation of the values of the pixels in the image. However, display, storage, retrieval, analysis, and distribution of multi-layer (or multi-band) digital data pose formidable problems, especially when the images consist of more than three data layers and contain more than a couple of hundred thousand pixels in each layer. Displaying such multi-layer data can be difficult because there are only three primary colors (or attributes), and each one of these colors can be displayed in at most sixteen different recognizable levels. Thus, reduction in the dimensionality of such data becomes an important aspect of digital image processing and presentation. Such multi-layer image data often exhibit high correlation among the layers, and hence the classical principal component analysis procedure (also known as the Karhunen-Loéve transform) may provide a new and smaller set of layers or image components that are generally uncorrelated with each other [1, 2]. These new layers (or principal components) can be ranked such that each new one has less variance than the preceding one. This ranking is carried out with the help of the eigenvalues of a dispersion matrix the elements of which are formed from the variance in each band and from the covariance among the bands.

As the variance of a principal component decreases with an increase of its order, the "information content" of the component generally decreases in a statistical sense. (Note that the phrase "information content" remains loosely defined.) Some investigators (e.g., [3]) have considered it prudent to keep all components for further analysis. Others, however, especially those primarily involved in the false color presentation of data [4-6] have implied that the higher-order components contain primarily noise and are therefore of no practical value. They then recommend the usefulness of the principal component analysis in reducing the dimensionality of multi-layer image data.

Considering the basic principles of principal component analysis, this position is understandable provided the image consists of a few major classes. In practice, however, an image can consist of several hundred thousand pixels with 10–20 different classes, some major and some minor. Under these circumstances, the belief that the higher-order components are insignificant may or may not be justified. For a false color presentation of multi-layer data, one can only work with three color attributes. In this case, the principal component transformation is a powerful tool, but its limitations must be recognized.

© Copyright 1982 by International Business Machines Corporation. Copying in printed form for private use is permitted without payment of royalty provided that (1) each reproduction is done without alteration and (2) the *Journal* reference and IBM copyright notice are included on the first page. The title and abstract, but no other portions, of this paper may be copied or distributed royalty free without further permission by computer-based and other information-service systems. Permission to *republish* any other portion of this paper must be obtained from the Editor.



Figure 1 Land use and land cover map of San Jose and vicinity.

Some of these statements [4-6] about principal components may result partly from limited experimentation on small images. That is, they were based on the number of pixels that can be handled on most stand-alone image processing systems or on those with image display hardware interfaced with a large computer in a "virtual-machine" environment. In contrast, we have used the recently announced IBM 7350, a 1024 × 1024-resolution, intelligent color display system with a local storage of about eight million bytes and an arithmetic logic unit for performing operations on the locally stored data. This device first became available within IBM in mid-1981 [7]. Devices for displaying still larger images have also been reported [8], and image processing devices capable of very-high-speed processing of such images can be expected to follow [9]. It therefore seems appropriate now to re-examine the information content aspect of principal component analysis.

The image processing and display device used for our investigations is attached to an IBM System/370 Model 158 computer running in the VM/CMS (Virtual Machine, Conversational Monitoring System) environment. This configuration provides easy access to large (about 100 megabytes) data files, and the capability of performing complex mathematical operations in the host computer if necessary.

A special feature (the random addresser for the refresh buffer) of the IBM 7350 enables the user to obtain a quick evaluation of a matrix whose $f_{i,j}$ element represents the number of pixels with the *i*th and *j*th radiance levels for the data stored in the *n*th and *m*th buffers, respectively. This matrix forms the basis for the generation of a three-dimensional histogram (bi-scatter plot) representing correlation between data in any two bands. It also assists in an efficient evaluation of the off-diagonal elements of the dispersion matrix representing the covariance of multi-band data; see Eqs. (1) and (2). We found the IBM 7350 to be especially convenient for this work because all hardware capabilities are made available to any application program written in a high-level language (e.g., FORTRAN).

In this paper, we discuss the results of our investigation on a 1024×1024 four-band (Landsat: MSS4 to MSS7), and on a 1024×1024 five-band (Landsat plus digital terrain elevation data) image of the Santa Clara Valley/Mt. Hamilton region of northern California. Selected original data and the corresponding principal component values are presented in the false color composites. Results of the multispectral classification on a few easily recognizable minor classes in the image are also presented in tabular form.

Image description

The region we selected for our investigation has diverse characteristics and features, including urban, suburban, recreational, forest, mountain, agricultural, and hydrological categories. A land use and land cover map of this general region (1974–1976 USGS map, open file 76-640-1) is shown in Fig. 1. Residential and commercial categories are shown in light yellow, while the urban land is shown in orange. Range and forest lands are shown in light and medium (or dark) green, respectively. Agricultural regions are shown in different shades of red, and water bodies are shown in black.

■ Landsat data

The Multi-Spectral Scanner (MSS) of the current Landsat series satellites scans the earth's surface in four spectral bands with a ground level resolution of about 80 m. These MSS data are now geometrically and radiometrically corrected and are transformed to one of several conventional map projections [10]. These partially processed MSS data are grouped into the so-called Landsat scenes of about 185 km (cross-track) by about 170 km (along-track). A scene consists of four bands with 2983 scan lines in each and with 3548 pixels per scan line. The spectral radiance of a pixel is represented in relative units by a 7-bit number (range: 0–127), which is stored in an 8-bit word.

The Landsat multispectral image used in our study was selected from the Landsat 3 scene containing the San Francisco Bay area (NASA scene ID: E-21529-17562-0; centered

at 37°21′ N, 121°47′ W; imaged on March 31, 1979). The selected image consists of 1024 lines, starting from the 1200th scan line in this scene, and 1024 pixels starting from pixel number 1350 from each selected scan line. Thus, there are 1 048 576 pixels in the image. The geographical coordinates for the corners of this image are (37.54° N, 122.03° W), (37.44° N, 121.38° W), (36.93° N, 121.51° W), and (37.03° N, 122.16° W) starting from the left top corner and proceeding in the clockwise direction.

• Digital terrain elevation data

Digital terrain data [11] generated from the 1:250 000-scale maps were used. Values of terrain elevation (in feet) are given on a 0.254-mm (0.01-in.) grid for 1°-latitude, 1°-longitude quadrangles. This resolution corresponds to about 61 m on the ground and compares well with that of the Landsat measurements. The positions of the digital data (i.e., grid points) are given in terms of the x, y map coordinates, and not in terms of latitude and longitude. The x, y coordinates of the four corners of the quadrangles were used to estimate the geographical location of a grid point. It may be noted that the latitude, longitude scales are slightly nonlinear.

In order to register the digital terrain elevation data on the Landsat scene, latitude and longitude of several ground control points easily identifiable on the Landsat scene and on the 1:250 000-scale maps were determined from the maps. The line and pixel numbers of these ground control points were then obtained [12]. Coefficients of a pair of equations relating the line-pixel parameters to the latitude-longitude parameters were calculated using the first two terms of the Taylor series for two variables. This mapping function was used to determine the latitudes and longitudes of all pixels in the Landsat scene. The terrain elevation for a Landsat pixel was determined by converting its latitude-longitude parameter into the x, y coordinates using all of the information provided for the corners of the corresponding quadrangle and by using the nearest-neighbor procedure.

The aforementioned re-sampling procedure is expected to provide registration of the terrain elevation data on the Landsat scene to within 2-3 pixels. Better registration is not practical because of the nonlinear relationship between the x, y coordinates and the latitude-longitude variables mentioned earlier and because of the discontinuities of the grid points at the boundaries of the quadrangle. However, this small degree of misregistration cannot invalidate any finding of this study.

The digital terrain elevation data cannot be contained in 8-bit numbers without scaling, since these values can, in general, range from 0 to 10 000 m. A full Landsat scene requires terrain data from several quadrangles of the

Table 1 Values of mean brightness (μ) and standard deviation (σ) for bands 4 to 8 of the image used in this investigation.

Band	Mean brightness	Standard deviation	
4	16.54	5.11	
5	17.55	7.02	
6	36.57	10.14	
7	36.17	11.60	
8	40.93	26.41	

1:250 000-scale maps. Therefore, we generated a terrain elevation data file in registration with the Landsat scene and containing 16-bit (half-word integer) numbers for each pixel. The elevation values in this file were found to vary between 0 and 1282 m. For merging the terrain data with the Landsat data, it was necessary to scale the data into 7-bit numbers. A second terrain elevation file was produced from the first one using a vertical scale factor of about 11 m. This second terrain elevation file is referred to as the "band 8 data" throughout this paper. Its count range varies from 8 to 127, with each count representing approximately 11 m in elevation.

Several shaded relief images of a part of the image used in this investigation can be found elsewhere [13].

Principal component transformation

The statistical parameters of mean brightness (μ) and standard deviation (σ) for all five bands of the image described in the preceding section are given in Table 1. The procedure for computing the principal component transformation matrix can be found in many textbooks on image processing (e.g., [1-4]) and hence is not described here in detail. It basically starts with a symmetric dispersion matrix whose main diagonal elements are given by σ^2 . The off-diagonal element $C_{k,m}$ representing the covariance of the data in the kth and mth band is defined by

$$C_{k,m} = \frac{1}{N} \sum_{n=1}^{N} (R_{k,n} - \mu_k) (R_{m,n} - \mu_m), \tag{1}$$

where $R_{k,n}$ ($R_{m,n}$) is the radiance of the *n*th pixel in the *k*th (*m*th) band. The upper limit *N* represents the total number of pixels in the image.

In order to perform the bulk of the computations in the IBM 7350 where the data reside, Eq. (1) was modified as follows for the 7-bit case:

$$C_{k,m} = \frac{1}{N} \sum_{i=0}^{127} \sum_{j=0}^{127} (i - \mu_k)(j - \mu_m) f_{i,j}, \tag{2}$$

where the quantity $f_{i,j}$ is as defined earlier near the end of the Introduction. After evaluation of all of the elements of the f_{ij}

717

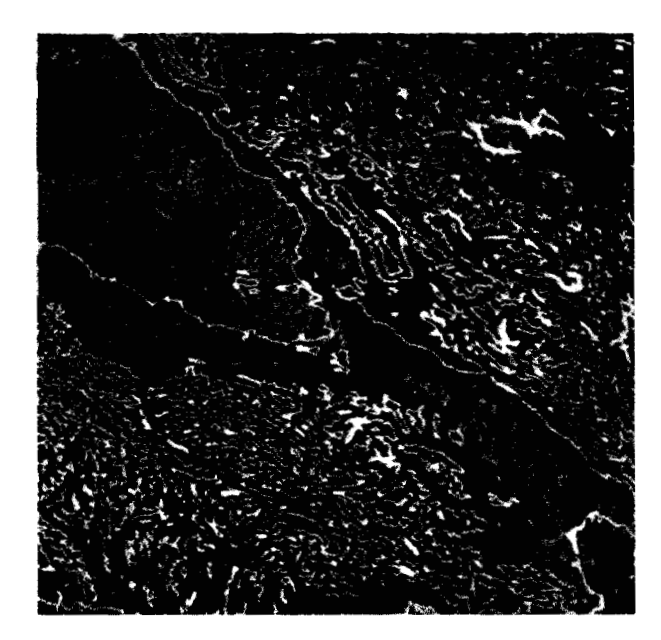


Figure 2 False color display of the original image data for the Santa Clara Valley/Mt. Hamilton region. Data for bands 4, 5, and 7 are shown in 16 different shades of blue, green, and red, respectively.

matrix in the IBM 7350, the quantity $C_{k,m}$ can be computed in the host (System/370) after reading the contents of the refresh buffer [12].

After all elements of the dispersion matrix have been computed, its eigenvalues and eigenvectors can be computed using the standard procedure. These eigenvectors provide elements for the principal component transformation of the original image data. The normalized eigenvalues of the dispersion matrix are frequently used to characterize the "information content" of the principal components.

The normalized eigenvalues of the four-band (bands 4 to 7) image are as follows: 0.754, 0.232, 0.010, and 0.005. The components P_1 , P_2 , P_3 , and P_4 of any pixel can be computed from the following equation:

$$\begin{bmatrix} \mathbf{P}_1 \\ \mathbf{P}_2 \\ \mathbf{P}_3 \\ \mathbf{P}_4 \end{bmatrix} = \begin{bmatrix} 0.1320 & 0.1586 & 0.6535 & 0.7283 \\ 0.5379 & 0.7667 & 0.0845 & -0.3402 \\ 0.0668 & -0.3815 & 0.7203 & -0.5754 \\ 0.8299 & -0.4914 & -0.2167 & 0.1510 \\ 0.8299 & -0.4914 & -0.2167 & 0.1510 \\ \end{bmatrix} \begin{bmatrix} R_4 \\ R_5 \\ R_6 \\ \end{bmatrix} + \begin{bmatrix} 1 \\ 18 \\ 50 \\ R_7 \end{bmatrix},$$
(3)

where R_4 , R_5 , R_6 , and R_7 are the radiances of the pixel in the four MSS bands.

The normalized eigenvalues of the five-band (bands 4 to 8) image are as follows: 0.715, 0.221, 0.060, 0.003, 0.001. The

components π_1 to π_5 of any pixel can be computed from the following equation:

$$\begin{bmatrix} \pi_1 \\ \pi_2 \\ \pi_3 \\ \pi_4 \\ \pi_5 \end{bmatrix} = \begin{bmatrix} -0.1016 & -0.1118 & -0.1250 & -0.0724 & 0.9779 \\ 0.0772 & 0.0955 & 0.6325 & 0.7488 & 0.1552 \\ 0.5195 & 0.7872 & 0.1150 & -0.2796 & 0.1380 \\ -0.0100 & -0.3141 & 0.7436 & -0.5900 & 0.0144 \\ \pi_5 \end{bmatrix} \begin{bmatrix} R_4 \\ R_5 \\ R_6 \\ R_7 \end{bmatrix} + \begin{bmatrix} 43 \\ R_6 \\ R_7 \end{bmatrix}$$

$$(4)$$

The second term in Eqs. (3) and (4) is for avoiding negative principal component values. The values of the elements of the P and π vectors are also treated as 7-bit data; if any element of any pixel exceeds the upper limit, it is forced to 127. It may be noted that because of this forcing and addition of the second term, these equations are not invertible explicitly.

From Eqs. (3) and (4), it is clear that the radiances of all bands contribute somewhat to the magnitude of a given component. However, generally two bands are prime contributors in each case. For discussion purposes, we can then make the following statements as a first approximation:

Vectors \mathbf{P}_1 and \mathbf{P}_2 are the weighted sums of R_6 and R_7 and of R_4 and R_5 , respectively. Similarly, \mathbf{P}_3 and \mathbf{P}_4 are the weighted differences of R_6 and R_7 and of R_4 and R_5 , respectively.

Vector π_1 essentially represents the band 8 data, *i.e.*, the terrain elevation information. Vectors π_2 and π_3 are the weighted sums of R_6 and R_7 and of R_4 and R_5 , respectively, while π_4 and π_5 are the weighted differences of the same two combinations.

Thus, in a qualitative manner, one can expect most information of the four-band image to be contained in the first two components and that of the five-band image in the first three components. The corresponding ordered eigenvalue sets also support this qualitative statement. However, this does not rule out the possibility of the last two components having some information.

Discussion of results

Results of our investigation are presented from two different viewpoints, viz., false color images and quantitative information related to and derived from the multispectral classification. For a false color presentation of multi-layer data, a histogram on a semi-logarithmic scale [14] was generated for each band. The histogram was then used to determine the count range containing about 99% of all of the pixels. A linear scale was then used to intensity-code pixels in this count range in 16 different shades of the appropriate primary color. Pixels to the left and pixels to the right of the count range were assigned the darkest and the brightest shade of

that color, respectively. For components P_3 , P_4 , π_3 , π_4 , and π_5 , using a count range with about 99% of all pixels resulted in an image strongly dominated by the color assigned to that component. It was therefore necessary to cut down the lower end of the range to obtain appropriate color balance.

A modified form of the "box-car" classification procedure (see, e.g., [12]) was used in our analysis. With this, the results are independent of the order in which the classes are specified. In this case, classes were numbered in the powers of 2, i.e., 1, 2, 4, 8, and so on. For training sites, areas consisting of about 220 pixels were used, and the count range containing 90% of all pixels was determined for each band of each class from the corresponding statistical information. If the values of a pixel in all bands lie in the corresponding count ranges of a given class, it is said to belong to that class. With the aforementioned numbering procedure, a mixed (or doubtful) pixel belonging to more than one class is assigned the number given by the sum of the number of these classes. For example, if a pixel is judged to belong to class 2 and class 4, it is assigned to class 6.

• False color presentation of the four-band data

The data for MSS bands 4, 5, and 7 are color coded into 16 different shades of blue, green, and red, respectively, and the resultant false color image is shown in Fig. 2. This is the conventional form of presenting Landsat data. Many features such as the bay, lakes, mountains, and residential areas can be easily identified. A comparison of Figs. 1 and 2 shows the usefulness of the Landsat series satellites in obtaining information about land cover and land use. The predominantly red color of the hilly regions is due to the presence of healthy vegetation with high reflectance in the near infrared.

In Fig. 3, results of the principal component analysis of the four-band data are presented with P_1 , P_2 , and P_3 values color coded in red, green, and blue, respectively. There is no standard convention for selecting colors for the principal component presentation, but it seems appropriate to use blue for the band with the least amount of information [2]; the human eye is less sensitive to blue. Almost all features of Fig. 2 are also present in Fig. 3 but in different colors.

The normalized eigenvalue corresponding to P_3 is 0.010 [see discussion for Eq. (3)], and hence its information content is about 1%. Furthermore, it represents primarily bands 6 and 7, which are already represented in an alternate manner by P_1 . However, if the P_3 data are deleted from Fig. 3, the visual separation between the rangeland (purple) and the forest land (brown and red) east and southeast of the San Jose area becomes less clear. Besides, there appears to be better separation of the agricultural and non-agricultural features with the additional component.

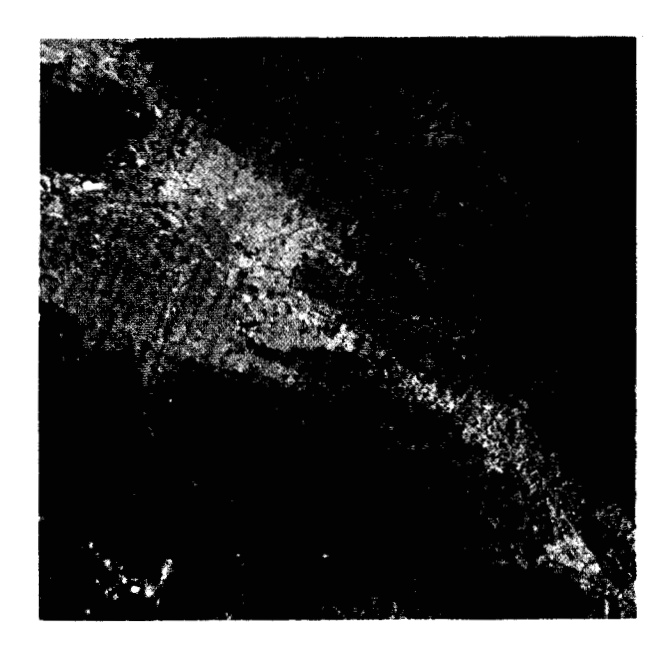


Figure 3 False color display of the principal components of the four-band data for the Santa Clara Valley/Mt. Hamilton region.

• Multispectral classification of the selected four-band data

The main purpose of this exercise is to examine the "information content" aspect of the higher-numbered principal components. It would be ideal to work with the image over a large area for which the "ground truth" at the time of measurement is known in great detail. Obviously, this becomes a major undertaking. Furthermore, the principal component transformation matrix can be expected to be dominated by the major classes of the image. Hence, one alternative to a large-scale experiment is to look at the importance of the higher-order components to the estimation of the number of pixels for minor classes.

The minor class which can be unambiguously identified in our image is water. It shows up in many parts of the image, at various elevations, in different depths, and with different amounts of impurities. It can also be verified, to some extent, from the land use map. For our multispectral classification exercise, we have selected three different training sites, all containing water. The Class 1 site is located in the southeastern part of the San Francisco Bay, which can be seen in the left top corner of Fig. 2 or 3. The Class 2 site is located in Calaveras Reservoir east of the bay. The Class 4 site is in Coyote Lake, which is situated on the extreme right in the lower part of the image. About 220 pixels were selected at each site, and the statistical characteristics of these limited data were obtained for all five bands. Values of the count range containing 90% of all pixels for each band of these

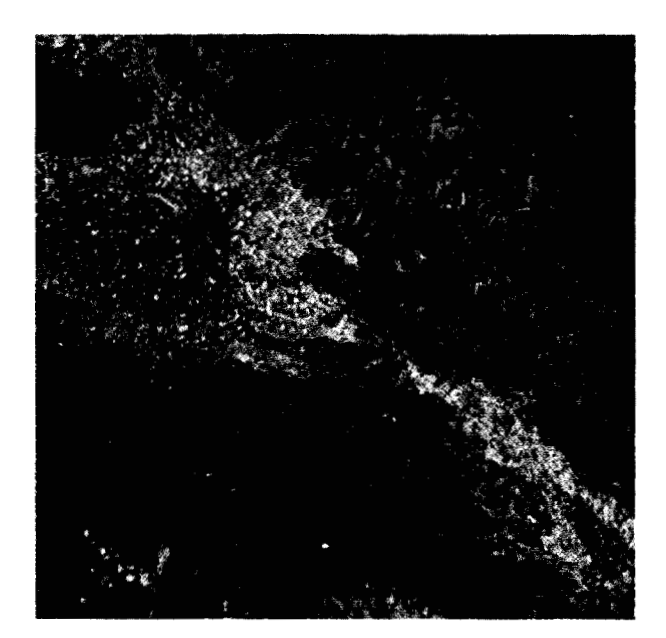


Figure 4 False color image of Fig. 2 with terrain-elevation contours.

Table 2 The 90% criterion count range for the original five-band data for three different training sites or classes: Class 1—Southeastern San Francisco Bay (225 pixels); Class 2—Calaveras Reservoir (225 pixels); and Class 4—Coyote Lake (213 pixels).

Band	90% criterion count range for			
	Class 1	Class 2	Class 4	
4	16-20	11-13	12-14	
5	11-15	8 - 10	10-11	
6	14-21	4-6	5-8	
7	1-6	0-1	0-2	
8	8 - 8	29-29	28-29	

Table 3 The 90% criterion count range for the four-band principal-component analysis case for three different training sites or classes: Class 1—Southeastern San Francisco Bay (225 pixels); Class 2—Calaveras Reservoir (225 pixels); and Class 4—Coyote Lake (213 pixels).

Component	90% ci	riterion count ra	inge for
	Class 1	Class 2	Class 4
1	15-23	6-8	8-11
2	35-40	30 - 32	32-34
3	54-58	50-52	50-52
4	21-24	21-23	20-22

classes are shown in Table 2 for the original data and in Table 3 for the four-band principal component data. The count ranges for Classes 2 and 4 overlap to some extent in

Table 4 Total number of pixels classified in each class with the original four-band data and with all four, the first three, the first two, and only the first principal component values for the Santa Clara Valley/Mt. Hamilton image.

Class number	Total number of pixels classified with				
	four-band data	P_1 to P_4	P_1 to P_3	P_1 to P_2	P, only
1	4363	4408	5051	6919	13647
2	935	651	890	1239	1353
4	709	873	909	1133	1522
6	178	58	119	134	667

some cases and thus provide conditions for the generation of a mixed class. For the results obtained with different principal component combinations, the number of pixels of a mixed class could change at the expense of those for the corresponding unique classes. One might then be able to supply some rationale for such a trend. However, results presented in this paper do not show such a trend.

The total number of pixels classified in each class over the entire image with the original four-band data and with the corresponding four principal components are shown in Columns 2 and 3 of Table 4, respectively. In both cases, the classified pixels show up in the expected geographic locations on the classification map. There are significant differences in the number of pixels identified by the original and the component data for a given class. However, there is no a priori reason to prefer one set of results over the other without some ground-truth information. The number of pixels in each class with only the first three, only the first two, and only the first component values are shown in the last three columns of this table. The number of pixels identified as belonging to a given class increase significantly even when the P₄ component with an eigenvalue of only 0.005 is suppressed. Furthermore, some of these newly identified pixels show up in areas with no water. Thus, it is clear that for this limited experiment, it is necessary to maintain all four components. In other words, no reduction in dimensionality is appropriate.

• False color presentation of the five-band data

Even though the terrain elevation information is contained in a single band, it is more predominant than the Landsat information. The validity of this statement can be visualized, to some extent, from the transformation matrix appearing in Eq. (4). The 16-bit terrain data can be presented in the overlay plane of the IBM 7350 color monitor in the form of elevation contours for the image in the image planes under it. Typical results are presented in Fig. 4 for the image of Fig. 2 with contours at 183-m (600-ft) intervals in the range 61-1281 m (200-4200 ft). Such a presentation can provide

great help to an interpreter involved in an interactive analysis of the data. However, it has very restricted use in hard copy production. A considerable amount of Landsat information is suppressed by about one-third of the terrain elevation data.

A false color composite with data for bands 5, 7, and 8, color coded into 16 different shades of green, red, and blue, respectively, is shown in Fig. 5. Because of the predominance of the terrain data, the Landsat information is considerably suppressed at higher elevation.

In Fig. 6, results of the principal component analysis of the five-band data are presented with π_1 , π_2 , and π_3 values color coded in red, green, and blue, respectively. A comparison of the results presented in Figs. 2 and 6 brings out the degree of enhancement that can be achieved by combining data from two different sources. The normalized eigenvalue corresponding to π_3 is only 0.060. But the herbaceous rangeland (light green) southeast of San Jose is separated from the urbanized area (medium blue) of San Jose in the threecomponent presentation (Fig. 6), while the two-component $(\pi_1 \text{ and } \pi_2)$ presentation results in a merging of these categories into a single (green color) combination. In addition, the π , component has introduced additional information and definition into the mountain regions. However, there appears to be some loss of road network information in the city area.

• Multispectral classification of the selected five-band data

Results similar to those given in Tables 3 and 4, but obtained with the five-band data, are presented in Tables 5 and 6, respectively. The discussion of the corresponding four-band case applies also to these results.

Concluding remarks

Principal component analysis has been shown to be a powerful tool for reducing the dimensionality of four-band and five-band data to three components. For our image, the third component for the four-band case carrying about 1% of the total information is found to be helpful in enhancing the value of the false color principal component presentation.

A modified "box-car" classification analysis was also performed for the unambiguously identifiable three different water classes in these images. These are the minor classes with the total number of pixels for a class measurable in hundreds. For such cases, our investigation brings out the need of working with all components in a quantitative extraction of information.

Reduction in the dimensionality of the multi-layer large images is a necessity, and the principal component analysis

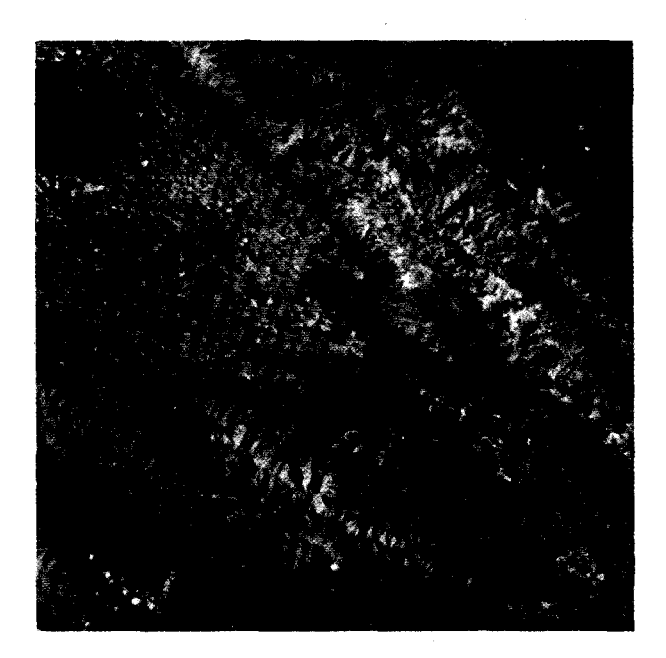


Figure 5 False color display of the original image and the terrain elevation data.

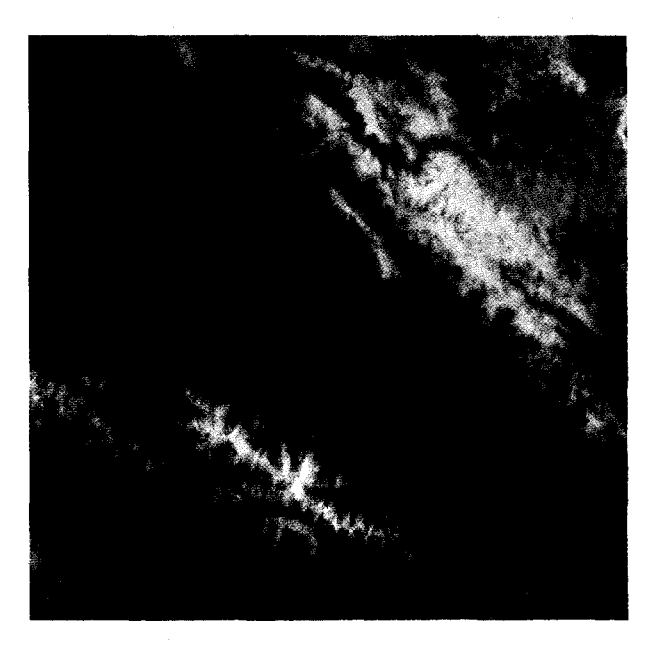


Figure 6 False color display of the principal components of the five-band data for the Santa Clara Valley/Mt. Hamilton region.

can assist in this task to some extent. Our study suggests that the extent depends upon several factors, such as the size of the image, number of classes in the image, their relative importance, number of bands or data layers, classes for which information is to be preserved by the components, and the nature of information to be extracted. Further investigation in this general direction is indicated.

Table 5 The 90% criterion count range for the five-band principal-component analysis case for three different training sites or classes: Class 1—Southeastern San Francisco Bay (225 pixels); Class 2—Calaveras reservoir (225 pixels); and Class 4—Coyote Lake (213 pixels).

Component	90% ci	iterion count ra	inge for
	Class 1	Class 2	Class 4
1	44-46	68-69	67–68
2	14-22	9 - 11	11-14
3	22-27	19-21	21-24
4	55-60	51 - 53	51-53
5	20-23	20-22	19-21

Table 6 Total number of pixels classified in each class with the original five-band data and with all five, the first four, the first three, and the first two principal component values for the Santa Clara Valley/Mt. Hamilton image.

Class number	Total number of pixels classified with					
	five-band data	π_1 to π_5	π_1 to π_4	π_1 to π_3	π_1 to π_2	
1	4358	5199	5546	6444	7814	
2	603	523	701	975	910	
4	321	290	295	343	376	
6	67	37	62	65	232	

References

- 1. Remote Sensing of the Environment, J. Lintz and D. S. Simonett, Eds., Addison-Wesley Publishing Co., Reading, MA, 1976.
- J. G. Moik, "Digital Processing of Remotely Sensed Images," NASA SP-431, U.S. Government Printing Office, Washington, DC, 1980.
- A. Fontanel, C. Blanchet, and C. Lallemand, "Enhancement of Landsat Imagery by Combination of Multispectral Classification and Principal Component Analysis," *Proceedings of the* NASA Earth Resources Survey Symposium 1-B, NASA TM X-58168, JSC-09930, 999-1012, 1975.
- R. O. Duda and P. E. Hart, Pattern Classification and Scene Analysis, John Wiley & Sons, Inc., New York, 1973.
- E. E. Triendl, "Landsat Image Processing," Advances in Digital Image Processing: Theory, Application, Implementation, Plenum Publishing Co., New York, 1978, pp. 165-175.
- A. Santisteban and L. Muñoz, "Principal Components of a Multispectral Image: Application to a Geological Problem," IBM J. Res. Develop. 22, 444-454 (1978).
- P. Franchi, "A System for Color Image Display and Processing," Scientific Center Report G513-3586, IBM Scientific Center, Rome, Italy, 1981.
- R. C. Tsai, "High Data Density 4-Color LCD System," Information Display, Society of Information Display, Los Angeles, CA, May 1981.
- P. D. Argentiero, J. P. Strong, and D. W. Koch, "Inventory Estimation on the Massively Parallel Processor," *Proceedings of* the 1980 Machine Processing of Remotely Sensed Data Symposium, LARS, Purdue University, West Lafayette, IN, 1980, pp. 286-298.
- Landsat Data Users Handbook, revised edition, U.S. Geological Survey, EROS Data Center, Sioux Falls, SD, 1979.

- Digital Terrain Tapes: NCIC User Guide, National Cartographic Information Center, U.S. Geological Survey, Reston, VA, 1978.
- J. V. Dave and R. Porinelli, "DIMAPS-II for IBM 7350," Scientific Center Report No. G320-3432, IBM Scientific Center, Palo Alto, CA, 1982.
- J. V. Dave and R. Bernstein, "Effect of Terrain Orientation and Solar Position on Satellite-Level Luminance Observations," Remote Sens. Environ. 12, 331-348 (September 1982).
- R. Bernstein, J. V. Dave, and H. G. Kolsky, "An Experimental Digital Image Manipulation, Analysis and Processing System (DIMAPS)," Scientific Center Report G320-3423, IBM Scientific Center, Palo Alto, CA, 1981.

Received April 14, 1982; revised June 9, 1982

Ralph Bernstein IBM National Accounts Division, 1501 California Avenue, Palo Alto, California 94304. Mr. Bernstein is at the Palo Alto Scientific Center and on the staff of IBM Fellow H. G. Kolsky. He joined the Center in 1979 and is currently involved in image processing. He joined IBM in the Federal Systems Division in 1956 in Owego, New York, and transferred to Gaithersburg, Maryland, in 1963. While in the Federal Systems Division, he was responsible for the management, analysis, design, and development of image processing technology and systems work under NASA and internal funding activities. He was a principal investigator on the NASA Landsat satellite program and led the development of advanced algorithms and programs for processing satellite image data. He received the NASA Medal for Exceptional Scientific Achievement and an IBM Outstanding Contribution Award for his effort. He managed the analysis of the development of a comprehensive satellite simulation, the Orbiting Astronomical Observatory (OAO). This simulation was used for ground operations personnel training, systems performance, and malfunction analysis. He was a member of a team that received a NASA OAO Group Achievement Award. Prior to that, Mr. Bernstein was involved in geophysical data acquisition and processing. He developed the first all-digital oceanographic data processing and control system for the Woods Hole Oceanographic Institution. At Owego, he was involved with inertial navigation system analysis and aircraft and submarine navigation system design and simulation. Mr. Bernstein has a B.S. in electrical engineering from the University of Connecticut, and an M.S. in electrical engineering from Syracuse University. He edited the book Digital Image Processing for Remote Sensing. Mr. Bernstein is a senior member of the Institute of Electrical and Electronics Engineers and a member of the Space Science Board of the National Academy of Sciences.

Jitendra V. Dave IBM National Accounts Division, 1501 California Avenue, Palo Alto, California 94304. Dr. Dave is at the Palo Alto Scientific Center, on the staff of IBM Fellow H. G. Kolsky. He joined IBM and the Center in 1967 and is currently involved in image processing science and applications. He has worked in atmospheric optics and radiative transfer, remote sensing of atmospheric ozone and aerosols, the effect of particulate contamination on climate, photovoltaic harvesting of solar energy, and large-scale scientific computing through FORTRAN. While on assignment to the Federal Systems Division, Dr. Dave worked on contracts to the NASA Goddard Space Flight Center, Greenbelt, Maryland, for investigations related to the estimation of ozone parameters from the Nimbus-G TOMS measurements. He was also a consultant to the Lawrence Livermore Laboratory, California, for atmospheric radiation transfer problems. Before joining IBM, Dr. Dave was a program scientist at the National Center for Atmospheric Research, Boulder, Colorado, from 1962 to 1967. He was also an Affiliate Associate Professor in the Department of Meteorology at the Florida State University, Tallahassee, from 1966 to 1968. He was principal investigator for the backscatter ultraviolet (BUV) experiment aboard the Nimbus-IV satellite from 1966 to 1967. From 1960 to 1962 he was a research scientist in the Department of Meteorology at Imperial College, London, England. He was a Visiting Assistant Professor and research scientist in the Department of Meteorology at the University of California, Los Angeles, from 1957 to 1960. From 1949 until 1957 he was a research assistant at the Physical Research Laboratory, Ahmedabad, India. Dr. Dave obtained his B.S. in physics and mathematics at Bombay University, India, in 1948, and his M.S. in physics in 1952. He received his Ph.D. in physics from Gujarat University, India, in 1957. Dr. Dave received an IBM Outstanding Contribution Award in 1972 for his work on the influence of atmospheric aerosols on the greenhouse effect.

Harwood G. Kolsky

IBM National Accounts Division, 1501
California Avenue, Palo Alto, California 94304. Dr. Kolsky, an IBM Fellow, is located at the Palo Alto Scientific Center. He is a

physicist who has been involved in a variety of projects including programming languages, scientific applications, and digital image processing. After seven years at the Los Alamos Scientific Laboratory, he joined IBM in 1957 at Poughkeepsie, New York, as a member of the product planning group for the Stretch computer. In 1959, he became assistant manager of the Federal Systems Division office in Omaha, Nebraska, Following this, he spent time at Federal Systems Division headquarters before being named manager of the Systems Science Department of the San Jose, California, Research laboratory in 1961. In 1962 he headed an advanced technology group in the Advanced Systems Development Division at Los Gatos, California. He joined the Palo Alto Scientific Center when it was formed in 1964 as manager of the atmospheric physics group. In 1968 he was named consultant and in 1969 an IBM Fellow. He served on the Corporate Technical Committee at Corporate Headquarters in Armonk, New York, from 1974 to 1975. He is head of the Board of Consultants for the IBM European Scientific Centers. Dr. Kolsky received his B.S. degree from the University of Kansas in 1943 and his Ph.D. in physics from Harvard University in 1950. Dr. Kolsky is a member of the American Physical Society, the Association for Computing Machinery, the Institute of Electrical and Electronics Engineers, and Sigma Xi.